LNF-94/057

An Infrared Synchrotron Radiation Beamline on DAΦNE

E. Burattini, G. Cappuccio, A. Marcelli, P. Calvani, A. Nucara,
M. Sànchez del Rìo

Nucl. Instr. & Meth. In Phys. Res. A 347, 308-312, (1994)

Nuclear Instruments and Methods in Physics Research A 347 (1994) 308–312
North-Holland

NUCLEAR
INSTRUMENTS
& METHODS
IN PHYSICS
RESEARCH
Section A

An infrared synchrotron radiation beamline on DAΦNE

E. Burattini [a,*], G. Cappuccio [b], A. Marcelli [c], P. Calvani [d], A. Nucara [d], M. Sánchez del Río [e]

[a] *INFN, Laboratori Nazionali di Frascati, 00044 Frascati, Italy; Università di Verona, Facoltà di Scienze, 37100 Verona, Italy*
[b] *CNR, Istituto Strutturistica Chimica, 00016 Monterotondo Scalo, Italy; INFN, Laboratori Nazionali di Frascati, 00044 Frascati, Italy*
[c] *INFN, Laboratori Nazionali di Frascati, 00044 Frascati, Italy*
[d] *Università di Roma "La Sapienza", Dipartimento Fisica, 00185 Roma, Italy*
[e] *European Synchrotron Radiation Facility, BP. 220, 38043 Grenoble, France*

DAΦNE, the new storage ring under construction at Frascati, can also be used as a powerful synchrotron radiation source in the infrared domain, where it is much more brilliant than a blackbody. Ray-tracing calculations of different optical setups at different wavelengths are reported.

Materials science, basic research in solid-state physics, electrochemistry, and other disciplines demand new radiation sources in the far-infrared. The sources should emit over the whole infrared (IR) band, to exploit the advantages of Fourier transform spectroscopy. They should also be much more brilliant than a blackbody, but not such that the linear response regime breaks down when interacting with the samples.

The interest in infrared synchrotron radiation (IRSR) as a possible probe dates from 1966, when a Solid State Panel of the National Research Council of the USA addressed the significance of synchrotron radiation as an IR source, particularly in the far IR [1]. However, only in 1973 was a specific study made by Stevenson et al. [2], while the first paper on synchrotron infrared emission measurements was published in 1976 [3]. Since then, SR sources have being increasingly considered by spectroscopists as a useful alternative to black bodies for far-IR spectroscopy.

In 1985, the first dedicated infrared synchrotron radiation (IRSR) beamline became operational at UVSOR (Okazaki, Japan) [4]. Other IR beamlines (see Table 1) from synchrotron dipolar magnets have since been built at Brookhaven, Berlin, Daresbury, and Lund. A beamline extracting IRSR from an undulator (SIRLOIN) has also been built at Orsay.

DAΦNE, the new storage ring under construction at Frascati, designed to be a meson factory, will operate at an energy of 0.51 GeV. The machine parameters (Table 2) make it suitable as an intense source of SR. Moreover, the expected performance of DAΦNE as a dedicated SR source is extremely interesting in the IR range. The unconventional DAΦNE layout (see Fig. 1) is discussed elsewhere [5]. Two rings with the same magnetic structure and optical functions cross on the horizontal plane at two points. Table 2 reports some of the design parameters of the DAΦNE project [5].

To calculate the beam dimensions σ_i ($i = x$, y where x is the horizontal axis and y the vertical axis) and the divergences σ_i' at four different source points – two bending magnets BLS and ELP, the wiggler WIG (see Fig. 1), and the center of the very long straight section where the interaction IP1 point is located – we use the DAΦNE parameters listed in ref. [5], the standard equations for the emittances (ϵ_i), and the dispersion (β_i) functions. The values reported in Table 3 are obtained by using the design emittance $\epsilon = 10^{-6}$ m rad and the design coupling coefficient $\kappa = 0.01$.

The vertical beam size σ_y and the divergence σ_y' (about 100 μm and 100 μrad, respectively) are satisfactory not only for the wiggler but also for both the bending-magnet sources. In fact, the vertical beam size is about twice the wiggler source value. However, due to the large natural emittance in the infrared, all the horizontal parameters are quite large. It is worth noting that the horizontal divergence of the second bending magnet BLP is three times smaller than that of the BLS.

From the above electron beam dimensions, we can calculate the vertical source characteristics at different wavelengths. The angular spread of the radiation in the vertical plane is

$$\sigma_Y' = \sqrt{\left(\sigma_{y'}^2 + \sigma_\psi^2\right)}, \tag{1}$$

where σ_ψ is the natural synchrotron radiation angular width (r.m.s.), which is a function of the ratio λ/λ_c. On DAΦNE, for the infrared and VUV emission ($\lambda/\lambda_c \gg 1$) [6],

$$\sigma_\psi(\text{mrad}) = 0.816(\lambda/\lambda_c)^{0.354}/E\ (\text{GeV}). \tag{2}$$

* Corresponding author.

SSDI 0168-9002(94)00476-N

For example, at a wavelength of 10 μm, the r.m.s. angular spread is greater than 20 mrad and increases with the wavelength. Such values make the $\sigma_{y'}$ contribution negligible compared to the divergences of Table 3 for both bending magnets and for the wiggler. This is a desirable situation for IR emission, because the effective source divergence angles in the horizontal and vertical plane (σ_x' and σ_y') are as small as possible and are determined only by the characteristic synchrotron emission.

The infrared photon flux has been calculated for a bending magnet and is reported in Fig. 2 (at $\lambda = 100$ μm and at $\lambda = 10$ μm) for both linear polarization components (σ, π) of the SR. Infrared radiation from DAΦNE, collecting 50 mrad on the horizontal plane at a current of 2 A, will be in the range 10^{14}–10^{15} photon/s per 0.1% bandwidth. These values are roughly the same as for SIRLOIN, which extracts radiation from an undulator [7].

IR radiation from the DAΦNE bending magnet is, therefore, extremely promising because of the intensity of the radiation that can be delivered. In our preliminary design, we started by considering the emission of a DAΦNE bending magnet collecting about 50 mrad on the horizontal plane and all the emission in the vertical plane. Our setup consists of a first plane mirror located close to

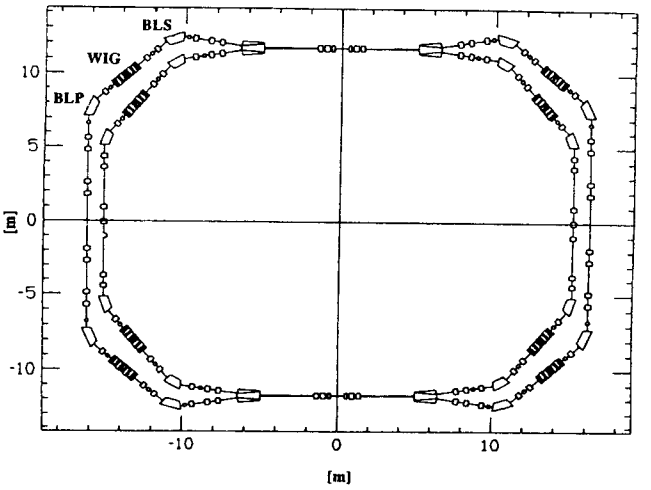

Fig. 1. Layout of the DAΦNE storage rings. SR sources (see text) are indicated as BLS, WIG and BLP.

Table 1
SR facilities with IR beamlines, including those proposed or under construction

Ring	Site	Status	Energy (GeV)	IR beamline	Emittance (m rad 10^{-9})
Max-1	Lund	in operation	0.55	operating	40
NSLS VUV	Brookhaven	in operation	0.75	operating	150
UVSOR	Okazaki	in operation	0.75	operating	160
SuperACO	Orsay	in operation	0.8	under test	37 (H)–18 (V)
Elettra	Trieste	under construction	1.5	proposed	4 (H)–0.4 (V)
SRS	Daresbury	in operation	2.0	under test	110 (H)
DAΦNE	Frascati	under construction	0.51	proposed	1000 (H)–10 (V)

Table 2
Parameters for a single DAΦNE ring

Energy E	510 MeV ($\gamma = E/mc^2 = 10^3$);
Bending magnet	$\rho = 1.4$ m, $\epsilon_c = 208$ eV, $B = 1.2$ T
Wiggler	$\rho = 0.94$ m, $\epsilon_c = 311$ eV, $B = 1.8$ T
Wiggler period length	0.64 m, $N_{period} = 3$
Momentum compaction	0.017
Natural horizontal emittance	10^{-6} m rad
vertical emittance	1.82×10^{-11} m rad
Natural horizontal chromaticity	−6.9
vertical chromaticity	−16.9
Coupling coefficient κ	0.01
Number of particles/bunch	9×10^{10}
Number of bunches	1–120
Max. total average current	5.3 A
RF frequency	368.25 MHz
Max. synchrotron radiation power/beam	49 kW
Relative r.m.s. energy spread	3.97×10^{-4}
Anomalous relative r.m.s. energy spread ($\Delta p/p$)	1.46×10^{-3}
Total single beam lifetime τ	~160 min

Table 3
Electron source size and divergence for DAΦNE at four different ring positions (see text)

Source	σ_x (mm)	σ_x' (mrad)	σ_y (mm)	σ_y' (mrad)
IP1	2.12	0.471	0.021	0.471
BLS	2.21	1.57	0.280	0.036
WIG	4.13	0.341	0.109	0.091
BLP	2.17	0.534	0.313	0.032

the orbit (~ 2 m), and set at 45° to deflect the radiation upwards. Since the mirror withstands the maximum power load, it has to be cooled. Preliminary studies of the cooling geometry are in progress.

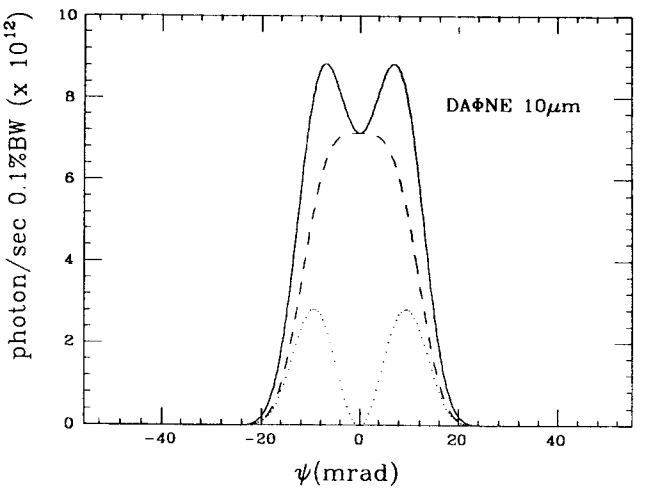

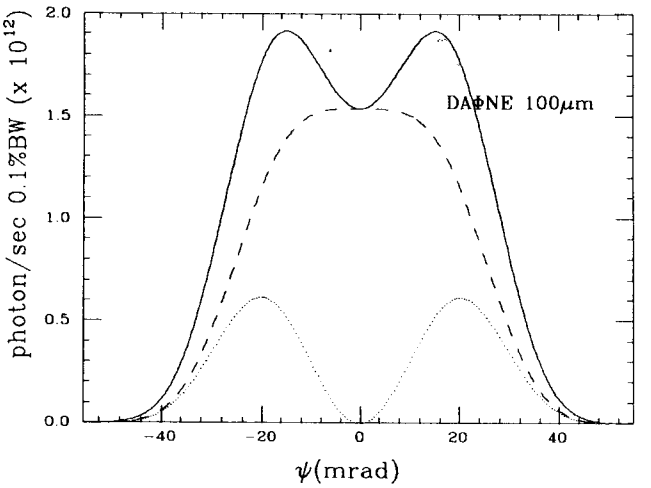

Fig. 2. Top panel: plot of the total flux emitted by the bending magnet of DAΦNE in the mid IR ($\lambda = 10$ μm), with 2 A of current and collecting 50 mrad of radiation on the horizontal plane (solid line). The dashed line is the component of radiation polarized on the plane of the ring (σ); while the dotted line is the perpendicular component (π). Bottom panel: the same at a wavelength of $\lambda = 100$ μm.

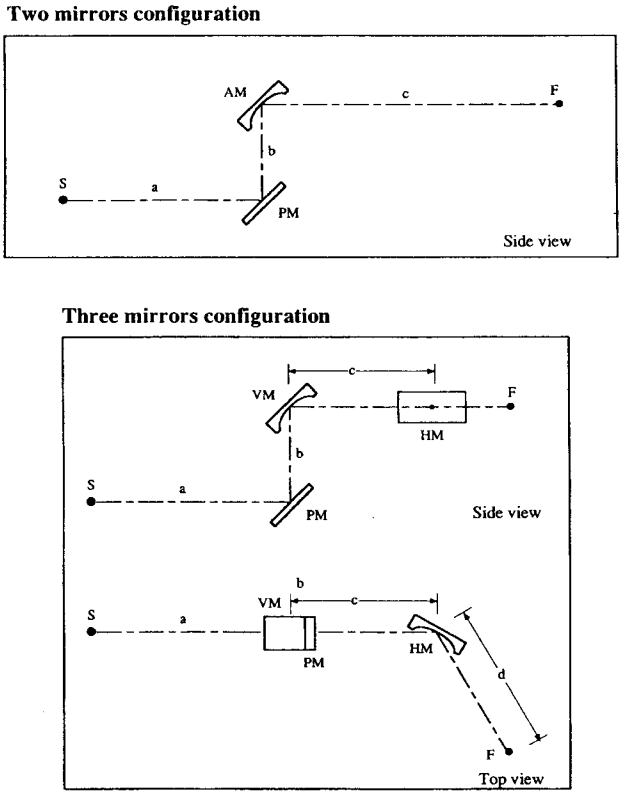

Fig. 3. Top panel: side view of the two-mirror optical configuration PM + AM (AM = aspherical mirror). S = source and F = focus image. Main parameters are in meters: $a = 2$, $b = 1$, while $c = 1.5$ ($m = 1/2$) or $c = 3$ ($m = 1$). Bottom panel: side view and top view of the three-mirror optical configuration PM + SM. (HM = horizontal mirror, VM = vertical mirror.) Main parameters are in meters: $a = 2$, $b = 1$, $c = 1.5$, and $d = 1.5$.

Radiation has to be focused onto a diamond window of about 1 cm diameter, placed at about 5 m from the source. The window separates the ultrahigh vacuum section connected to the front end of the ring from the low-vacuum section connected to the interferometer. Focusing at the entrance slit of the instrument will be performed by an additional optical setup not discussed here.

The transfer optics of the beamline has been calculated by ray-tracing procedures. The calculations were performed by means of SHADOW [8] at two different wavelengths: 50 μm and 1000 μm. To optimize the transmission through the window and to obtain the best image of the source, we considered two different schemes:

i) With two mirrors: the first mirror is plane (PM), while the second is aspherical, either toroidal (TM) or ellipsoidal (EPM) (see Fig. 3, top panel). The calculations were performed at two different magnifications: $m = 1$ and $m = 1/2$;

ii) With three mirrors: the first is a PM and the other two are spherical mirrors (SM) in a Kirkpatrick–Baez geometry for independent vertical and horizontal focusing. The calculations were performed with a magnification

Table 4
Results of ray-tracing calculations for different optical configurations. The numbers presented here show the main spot size (values are FWHM) and the relative intensity from a source of 5000 rays. ρ represents the flux density at the spot size ($\rho = N/(HV)$). H = horizontal spot size, V = vertical spot size, m = magnification

	(m)	50 μm				1000 μm			
		H (cm)	V (cm)	N (rays)	ρ (10^3)	H (cm)	V (cm)	N (rays)	ρ (10^3)
2-mirror configuration									
TM	(1/2)	0.52	0.13	5000	73.9	0.56	0.11	3529	57.3
EPM	(1/2)	0.50	0.032	5000	312.5	0.50	0.053	3530	133.2
TM	(1)	0.98	0.073	5000	69.9	0.97	0.11	3531	33.1
EPM	(1)	0.98	0.061	5000	83.6	0.97	0.087	3531	41.8
3-mirror configuration									
$SM^V(1)$	$SM^H(1/3)$	0.53	0.047	3073	122	0.58	0.067	2157	55.5
$SM^V(1)$	$EM^H(1/3)$	0.34	0.046	3074	196.5	0.35	0.067	2157	92.0
$SM^V(1)$	$SM^H(1/3)$					1.041	0.085	3529	40.0
$SM^V(1)$	$EM^H(1/3)$					0.34	0.086	3529	120.7

$m = 1$ for the vertical (V) focus and $m = 1/3$ for the horizontal (H) focus (bottom panel of Fig. 3). In case ii), calculations replacing the horizontal focusing mirror with an elliptical mirror (EM) were also carried out. The parameters to be compared are the focus spot size produced by different optics and their integrated intensities at the focal point.

The intensities are highly dependent on the mirror dimensions. Some results are reported in Table 4, which shows the horizontal and vertical sizes of the focus spot (in cm): N is the number of rays collected in the image point area, the ρ parameter is the flux density at the image point (i.e., rays/cm^2), as obtained from the ray-tracing results, and allows different images to be compared. The starting value is 5000 rays for all the calculations. The reflectivity of the mirrors is assumed to be 100%. In the table, numbers smaller than 5000 mean that some rays are lost by the optical system. For instance, at 1000 μm, the first PM does not collect all the vertical divergence of the source due to the slot of the bending magnet antechamber [9]. Preliminary conclusions can be drawn from the ray-tracing data. The widest image spots are those of the toroidal mirrors. Nevertheless, the TM gives acceptable shape and size for the $m = 1$ configurations. Aberrations give unacceptable images for the $m = 1/2$ magnification at both wavelengths.

The results obtained by replacing a TM with an EPM are very good: for the $m = 1/2$ configuration, the major semi-axis is 225 cm and the minor semi-axis is 150 cm. For the EPM the images are homogeneous and the flux densities (ρ) are greater ($\sim 20\%$) than those for the TM design, at both the wavelengths used here (see Table 4).

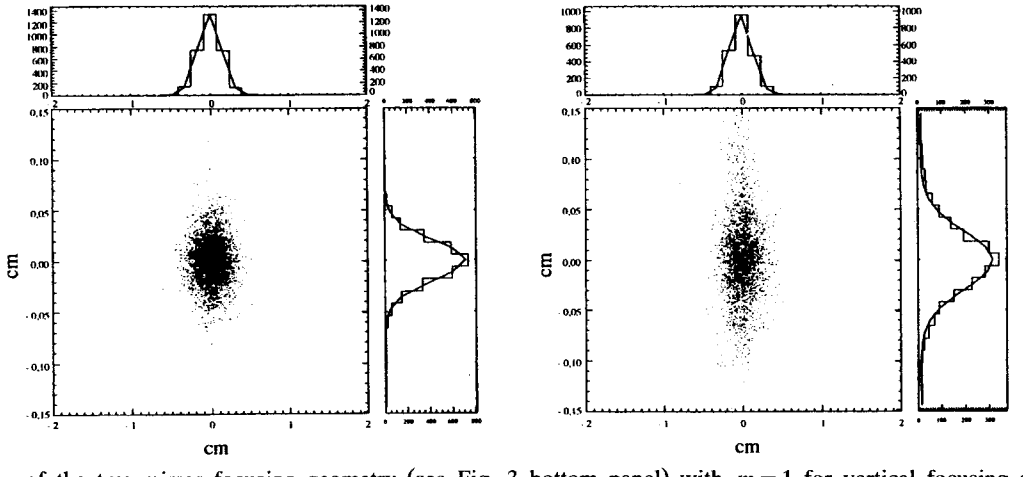

Fig. 4. Ray-tracing of the two-mirror focusing geometry (see Fig. 3 bottom panel) with $m = 1$ for vertical focusing and $m = 1/3$ for horizontal focusing. Left panel $\lambda = 50$ μm. Right panel $\lambda = 1000$ μm. In this calculation the vertical mirror is spherical (SM), while the horizontal mirror is elliptical (EM).

When comparing the two-mirror configuration, the EPM is found to give the best performance. The only disadvantage of this choice is its high cost. An alternative may be offered by spherical mirrors. It is interesting to compare the performances of two SMs having independent focusing geometry with those of a system where the second mirror (H) is replaced by an elliptical mirror. This should improve the quality of the horizontal focusing by reducing spherical aberrations. One finds that the spot dimensions are similar to those of the EPM, or even better (in the horizontal plane), due to a different horizontal demagnification ($m = 1/3$). The spherical aberration of the optical configuration with two spherical mirrors almost disappears replacing the second SM with an EM (Fig. 4). However, the transmitted flux is substantially reduced in this geometry because the angle of incidence for the horizontal mirror has to be set at 70° to reduce lateral deflection. If one wishes to reflect all the radiation from this surface, the mirror length has to be increased up to ~ 80 cm. However, a longer SM will not produce any improvement, due to the simultaneous increase of spherical aberration. In this case, the second longer mirror has to be an EM to achieve complete reflection and a high-quality image. Summarizing, both the two-mirror (PM + EPM) and the three-mirror configurations (PM + SM + EM) produce good images. The final selection will take into account costs, including those of vacuum vessels and mechanical devices.

In conclusion, the DAΦNE SR sources (i.e., bending magnets and wiggler) are more intense and more brilliant than blackbody sources of radiation, both in the far and the mid infrared regions. Even if insertion-device sources are more attractive for several reasons [7,9], at this early stage of the DAΦNE project, extraction of IR radiation from a bending magnet would seem to be more suitable. Although IRSR has a large natural divergence and the source is considerably extended in space, a suitable transfer optics is shown to produce a small brilliant spot.

References

[1] F.C. Brown et al., Synchrotron radiation as a source for the spectroscopy of solids, NRC Solid State Panel Subcommittee Rep. (1966)
[2] J.R. Stevenson, H. Ellis and R. Bartlett, Appl. Opt. 12 (1973) 2884.
[3] P. Meyer and P. Lagarde, J. Phys. 37 (1976) 1387.
[4] T. Nanba, Y. Urashima, M. Ikezawa, M. Watanabe, E. Nakamura, K. Fukui and H. Inokuchi, Int. J. Infrared Millim. Waves 7 (1986) 1769.
[5] M. Bassetti, M.E. Biagini, C. Biscari, S. Guiducci, M.R. Masullo and G. Vignola, DAΦNE Technical Note L-1 (1991); M.E. Biagini, S. Guiducci, M.R. Masullo and G. Vignola, DAΦNE Technical Note L-4 (1991); DAΦNE Machine Project, LNF-92/033 (P) (1992).
[6] X-ray Data Booklet, Center for X-ray optics, Lawrence Berkeley Laboratory, University of California.
[7] P. Roy, Y.-L. Mathis, A. Gerschel, J.-P. Marx, J. Michaut, B. Lagarde and P. Calvani, Nucl. Instr. and Meth. A 235 (1993) 568; Y.-L. Mathis, private communication.
[8] B. Lai and F. Cerrina, Nucl. Instr. and Meth. A 246 (1986) 337.
[9] A. Marcelli and P. Calvani, LNF Internal Report 93/027 (IR).